Improved Calculation of Li and Na Intercalation Properties in Anatase, Rutile and TiO_2(B)

J. A. Dawson and J. Robertson

Department of Engineering, University of Cambridge, Cambridge CB2 1PZ, United Kingdom

ABSTRACT

In recent years, TiO_2, as a potential electrode material in Li and Na batteries, has been the subject of considerable experimental and computational research. However, the typical density functional theory (DFT) functionals used (e.g. the generalised gradient (GGA)) for such calculations are not without their shortcomings. To avoid these well-known issues, we report the first use of hybrid DFT calculations to calculate the Li and Na intercalation properties for anatase, rutile and TiO_2(B). The magnitude of GGA intercalation voltage underestimation is shown to vary depending on the polymorphs. We find that Li intercalation is most energetically preferred in anatase, while Na intercalation is most feasible for TiO_2(B). Using the screened exchange hybrid functional, all intercalation processes are shown to be thermodynamically favourable, with the exception of Na in rutile. The electronic structures of these intercalated materials are also calculated and significant improvements, in terms of band-gap prediction and charge localisation, are presented in comparison to GGA. We hope that our results will encourage more use of hybrid density functionals in the modelling of fundamental battery material properties.

Electronic mail: j.a.dawson@bath.ac.uk

1. Introduction

The ongoing search for new, cheap, safe and more efficient battery materials to quell the ever rising demand for portable and large-scale energy applications has led to tremendous amounts of research[1-4]. In particular, TiO_2-based materials have proven to be popular in this search as a result of their low cost, light weight and nontoxicity[5,6]. Numerous TiO_2 polymorphs have been investigated, both experimentally and computationally, for their performance as battery anodes and ability to incorporate Li and Na ions. It has been shown that nanoscale and nanoporous TiO_2 can incorporate more Li and Na electrolytes compared to the respective bulk materials, resulting in high cycle life and improved charge density from the suppressed formation of the solid electrolyte interphase[7-9]. An understanding of the behaviour of the intercalated metal ions in a host material is essential to understanding its electrochemical performance and for the development of new and improved battery materials.

Anatase, rutile and TiO_2(B) have all been examined for their potential application in Li- and Na-based battery materials and a wide range of results has been reported. It has been experimentally confirmed that anatase can readily incorporate Li[5,8-10]. For Na, however, the situation is not as clear and is dependent on the TiO_2 nanostructure. Xiong et al.[11] tested nanowire TiO_2 grown on a Ti substrate, but only a low maximum capacity was achieved and it was concluded that anatase was inactive in their cell. Alternatively, for Na-intercalated nanocrystalline anatase[12] and anatase nanorods[13], excellent cyclability and high-rate capabilities were reported. Furthermore, in a recent study[14], it was shown that Na-intercalated anatase TiO_2 has a higher capacity and superior cycling, compared to amorphous and rutile TiO_2. Such a contradiction is an example of where computational studies can assist in the development of an understanding of the insertion process in such materials. As discussed, intercalation into bulk anatase samples is limited by a number of factors including phase

separation, whereas nanostructured samples can access stoichiometries that are usually unstable in the bulk, potentially allowing for increased charge densities[15-17].

Li intercalation is also possible for rutile[18-20], although it is well known that it cannot intercalate as much as Li as the anatase phase, although nanostructuring can again significantly improve this issue[18]. As a result of this limitation, there has been less research interest focused on rutile, compared to anatase and TiO_2(B). With regards to Na intercalation, sodiated rutile can be formed, but its electrochemical activity is poorer than that of anatase[14]. In a recent study[21], however, rutile microspheres, anchored by nanoneedle clusters, have been shown to exhibit good energy storage behaviour. The authors also suggest that rutile TiO_2 could be a new promising candidate for anodes in Na ion batteries. TiO_2(B) is lower in density than anatase and rutile and is therefore an excellent host material for intercalation[22,23]. For example, Li-intercalated TiO_2(B) nanowires have been shown to produce electrochemical properties[22]. The relatively open tunnel structure of TiO_2(B) also means that it can incorporate Na and when it is produced in the form of nanotubes, it has good cycle stability and high rate performance[23]. Good electrochemical performance has also been reported for Na-intercalated TiO_2(B)/graphene nanocomposite anodes[24]. Even from this short summary of the literature concerning Li and Na intercalation in TiO_2, it is clear that there is a significant amount of contradictory experimental results and that the intercalation and electrochemical performance of these materials is highly dependent on their nanostructuring.

These three TiO_2 polymorphs have also been considered in density functional theory (DFT) studies. Morgan and Watson[15] used the generalised gradient approximation (GGA) with the Hubbard *U* correction to calculate Li intercalation into anatase. They found good agreement with the experimental values for the intercalation energy and interoctahedral diffusion. For rutile, Li intercalation has also been shown to be energetically favoured[25], although not to the

same extent as anatase[26]. Using a variety of DFT functionals, Morgan and Madden[27] studied Li intercalation in TiO_2(B). It was discovered that the GGA and local density approximation (LDA) predict the same general behaviour, but both fail to give the correct electronic structures. Dalton et al.[28] combined DFT and Monte Carlo simulations to study the thermodynamics of Li intercalation in TiO_2(B). They calculated that Li intercalation is thermodynamically favourable up to a Li/Ti ratio of 1.25, higher than the theoretical maximum usually assumed for TiO_2. Alternatively, computational studies of Na intercalation in these polymorphs is limited. Li, Na and Mg intercalation were considered in anatase, rutile, TiO_2(B) and amorphous TiO_2 using the Perdew-Burke-Ernzerhof (PBE) functional[29]. In this comparative study, intercalation energies were calculated for each polymorph using each intercalating metal and it was found that every type of intercalation was favourable, with the exception of Na intercalation in rutile.

Nearly all of the DFT studies on this topic use the LDA or GGA, which have both been shown to underestimate intercalation energetics[30] and fail in reproducing several other structural and electronic properties of the host materials. They are also well-known for their severe band-gap underestimation and inaccuracies in the calculation of defect transition levels. While some of these errors can be reduced using post-DFT methods like the inclusion of the Hubbard *U* parameter, they are often fitted for the desired purpose and it is not clear whether they are sufficiently accurate in predicting defect levels[31,32].

To correct for the problems associated with local-density methods, in this work, we use the screened exchange (sX) functional for the calculation of Li and Na defect formation energies, charge transitions and electronic structures in anatase, rutile and TiO_2(B). The sX functional has the major advantage of replacing all LDA exchange with a Thomas-Fermi screened Coulombic exchange potential. The local exchange and correlation functionals underlying the LDA and GGA cause spurious self-interaction which increases the energy of occupied states

and decreases the energy of unoccupied states, whereas the exchange potential is self-interaction free. This results in more accurate intercalation energies and charge transition levels. The sX functional has previously been successfully applied to TiO_2[33,34] and other metal oxides[31,32,35,36]. In calculations of intrinsic defects in both anatase[33] and rutile[33,34], the sX functional achieved excellent agreement with experiment in terms of the band-gaps, defect localisation and energetics. It should be noted that to some extent, TiO_2 is an ideal case for examining the differences between the results from hybrid and standard functionals as a result of the d electrons, which are particularly affected by the self-interaction error.

2. Methodology

All calculations were completed using the CASTEP plane-wave density functional theory code[37]. The sX calculations were completed using norm-conserving pseudopotentials for Ti, O, Li and Na, with the Ti and O pseudopotentials being generated by the OPUIM method[38]. A plane-wave cutoff energy of 750 eV was used for the sX calculations. The Thomas-Fermi screening length was set to 2.15 $Å^{-1}$ for all the TiO_2 polymorphs. This value has previously been proven to be appropriate for rutile TiO_2[34] and was chosen with consideration of the experimental band-gap of the material. For comparison, we also used GGA calculations with ultrasoft pseudopotentials and the Perdew-Burke-Ernzerhof (PBE) functional[39]. The valence electrons in these calculations were described by a plane-wave basis set with an energy cutoff of 500 eV. For anatase, a supercell containing 108 atoms with 3 x 3 x 1 unit cells was used for intercalation calculations. A 96 atom supercell consisting of 2 x 2 x 4 unit cells was used for rutile and a 96 atom supercell consisting of 1 x 2 x 2 unit cells was used for TiO_2(B). The internal geometries were relaxed within both sX and GGA using a single *k*-point at the Γ point and a 2 x 2 x 2 *k*-point mesh, respectively.

The defect formation/intercalation energy, H_q, as a function of Fermi energy (ΔE_F) from the valence band edge (E_V) and the relative chemical potential ($\Delta\mu$) of element α, can be calculated from the total energies of the defective supercell (E_q) and the perfect supercell (E_H) using the following formula:

$$H_q(E_F, \mu) = [E_q - E_H] + q(E_V + \Delta E_F) + \sum_{\alpha} n_{\alpha}(\mu_{\alpha}^0 + \Delta\mu_{\alpha}), \qquad (1)$$

where qE_V is the change in energy of the Fermi level when charge q is added and n_α is the number of atoms of species α. The Li and Na chemical potentials (μ_{Li}/ μ_{Na}) were calculated using body-centred cubic Li and Na metal unit cells, respectively. The metal-rich (O-poor) limit is assumed in all our calculations. Defect charge transition levels are not affected by chemical potentials.

3. Results and discussion

3.1. Undoped TiO_2 polymorph properties

The crystal structures of anatase, rutile and TiO_2(B) are shown in Fig. 1. Anatase TiO_2 belongs to the $I4_1/amd$ space group. In the structure, oxygen atoms form edge-sharing distorted octahedra, half of these octahedra are occupied by Ti atoms, while the other half are vacant and can act as potential intercalation sites. In nature, rutile is the most common form of TiO_2 and it adopts the $P42/mnm$ space group. The TiO_6 octahedra in rutile share edges in the *c* direction and corners in the *ab* planes. The space between occupied octahedra, used for Li and Na intercalation, is smaller in rutile compared to anatase. The TiO_2(B) structure is a member of the $C2/m$ space group and is composed of edge- and corner-sharing TiO_2 octahedra. This structure has three distinct sites available for the intercalation of ions.

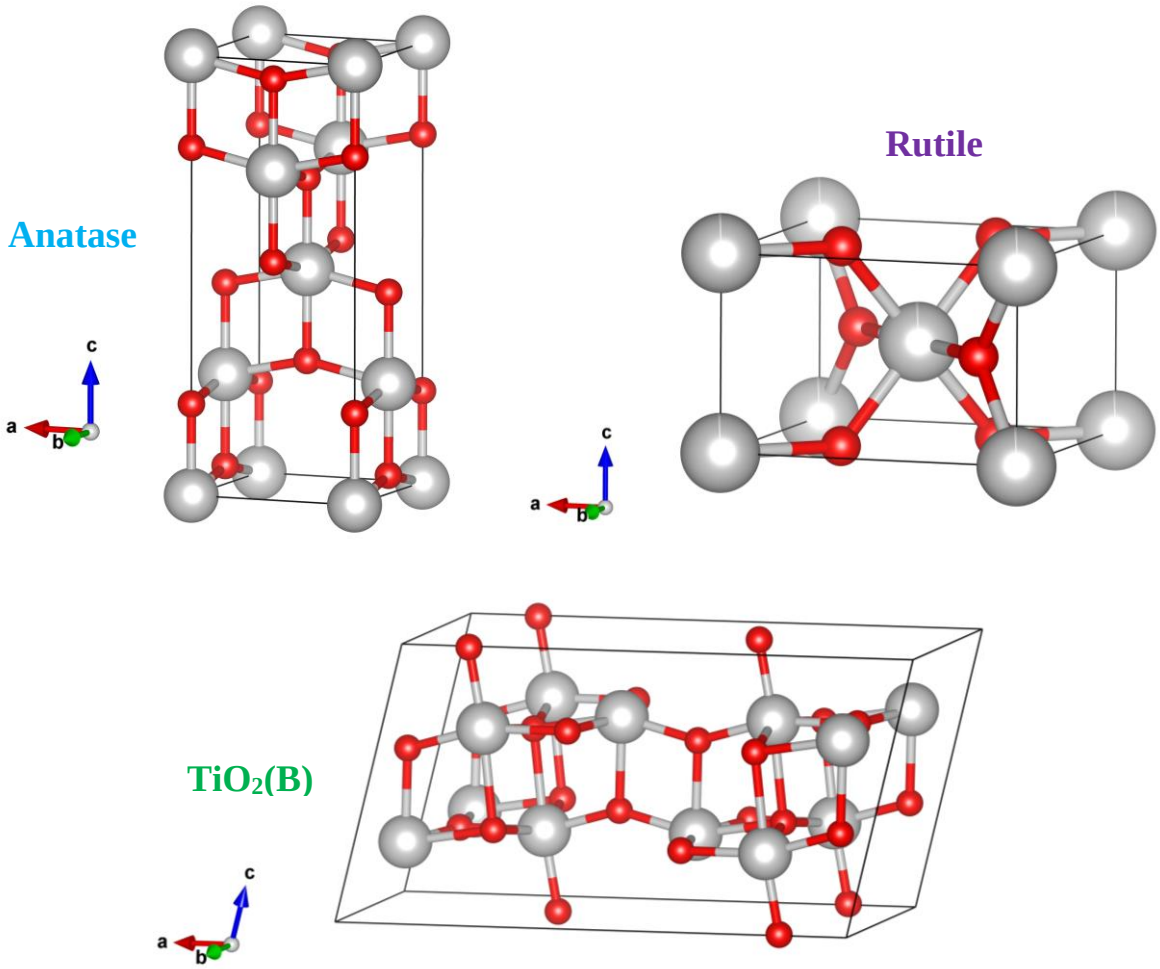

Fig. 1. Crystal structures of anatase TiO_2, rutile TiO_2 and TiO_2(B). Red and silver spheres represent oxygen and Ti atoms, respectively.

Table 1. Calculated and experimental lattice parameters for the three TiO_2 polymorphs. All lattice parameters are given in Å.

Structure	sX			GGA			Experiment[40,41]		
	a	*b*	*c*	*a*	*b*	*c*	*a*	*b*	*c*
Anatase	3.75	3.75	9.59	3.80	3.80	9.68	3.79	3.79	9.51
Rutile	4.56	4.56	2.96	4.63	4.63	2.96	4.59	4.59	2.96
TiO_2(B)	12.15	3.72	6.48	12.26	3.75	6.60	12.18	3.74	6.53

The lattice parameters for the three TiO_2 polymorphs, calculated using sX and GGA, are given in Table 1, experimental values are also provided for comparison. It can be seen that both the functionals are capable of reliably reproducing the TiO_2 structures. While the GGA tends to marginally overestimate the lattice parameters, the sX functional somewhat underestimates the values. Overall, the sX functional generally reproduces the structures more accurately compared to the GGA. However, it is noteworthy that the GGA lattice parameters calculated in this work are a significant improvement on some of the values previously reported[15,27,42,43]. The results for the sX calculated lattice parameters of rutile are in perfect agreement with the previous study[34]. Unfortunately, to the best of our knowledge, there are no previous sX calculations of bulk anatase or TiO_2(B) to compare to.

The partial density of states (PDOS) for the three studied TiO_2 polymorphs, calculated using the GGA and sX functionals, are plotted in Fig. 2. The valence bands of these structures are mostly made up of O 2p states with a high effective mass, whereas the conduction bands are mostly made up of Ti 3d states. As illustrated by Fig. 2, excess electrons in these materials will be centred on the d states of the cations, whereas electron holes are centred on the 2p states of the anions, consistent with electron paramagnetic resonance data[44]. The GGA calculated band-gaps for anatase, rutile and TiO_2(B) are 2.04, 1.77 and 2.57 eV, respectively. As expected, all three materials suffer from significant band-gap underestimation compared to the experimental values, although the underestimation is smaller for TiO_2(B). These values agree well with previous GGA calculations[45-47]. For sX, the calculated band-gaps are 3.51, 2.94 and 3.71 eV for anatase, rutile and TiO_2(B), respectively. Experimentally, the band-gaps for anatase, rutile and TiO_2(B) are 3.20, 3.03[44] and 3.22 eV[48], respectively. Clearly, sX reproduces the band-gaps of these polymorphs better than GGA, although there is some overestimation for anatase and TiO_2(B). Band-gap overestimation for some TiO_2 polymorphs has also been shown for GW

calculations[45]. Our sX calculated band-gaps are in excellent agreement with those previously calculated using the Heyd-Scuseria-Ernzerhof (HSE) hybrid functional[49-52].

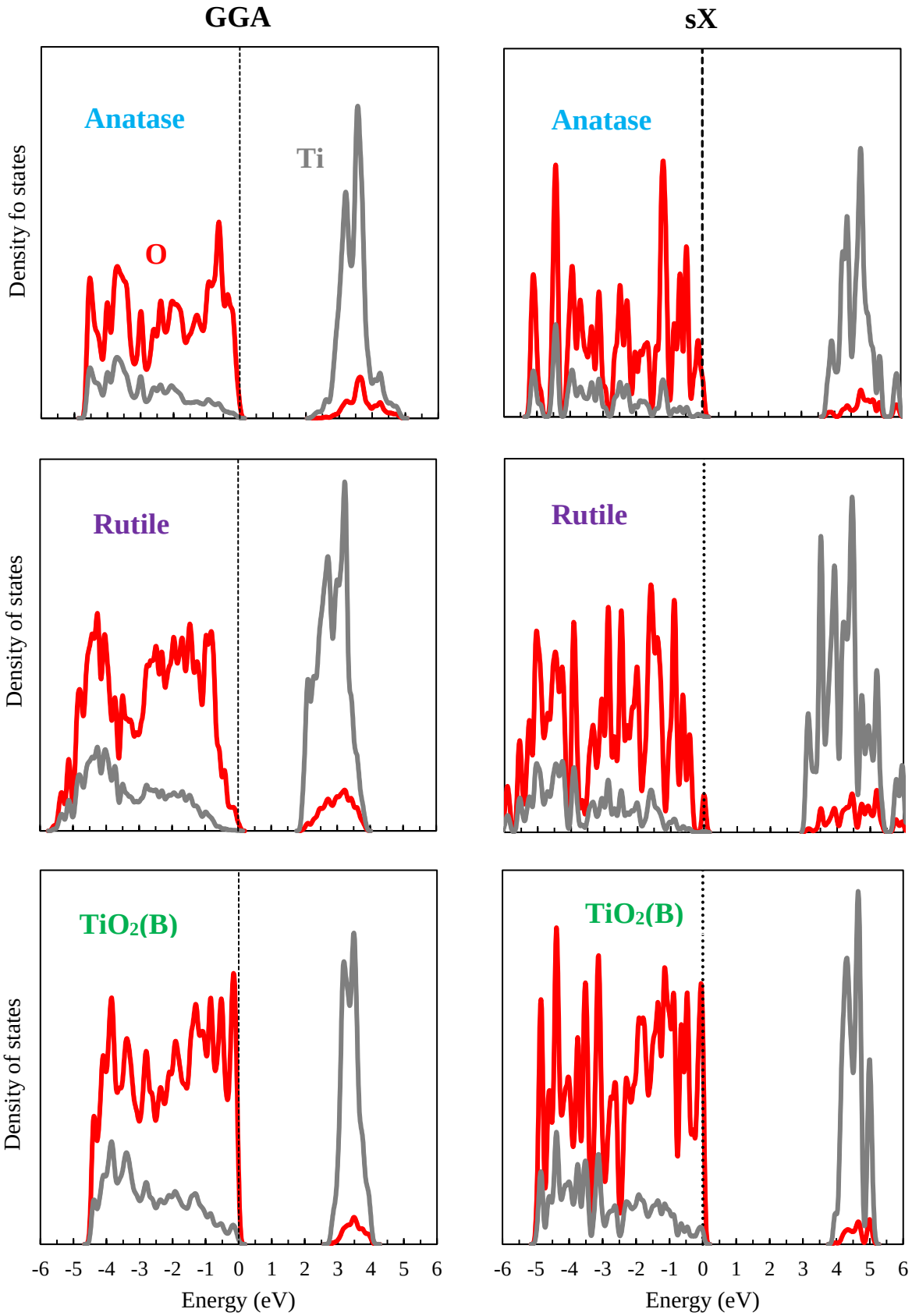

Fig. 2. PDOS of the three TiO_2 polymorphs calculated using the GGA and sX functionals.

3.2. Li/Na insertion sites

Li and Na can potentially occupy both the empty tetrahedral and octahedral sites in the anatase and rutile structures, although it is generally considered that the octahedral sites are energetically preferable, which is confirmed in this work also with the octahedral sites being favoured by -0.39 and -0.61 eV in anatase and rutile, respectively. For TiO_2(B), three intercalation sites have been proposed[53]. The C site is at the middle of a distorted octahedral site, while the A1 and A2 sites are 5-fold coordinated to oxygen atoms. The A1 site is displaced from the C site along the *c*-axis and is coordinated with oxygen atoms in the (001) plane, while the A2 site is displaced from the C site along the *a*-axis and lies between bridging oxygen atoms in the (001) plane. These sites are illustrated in Fig. 3.

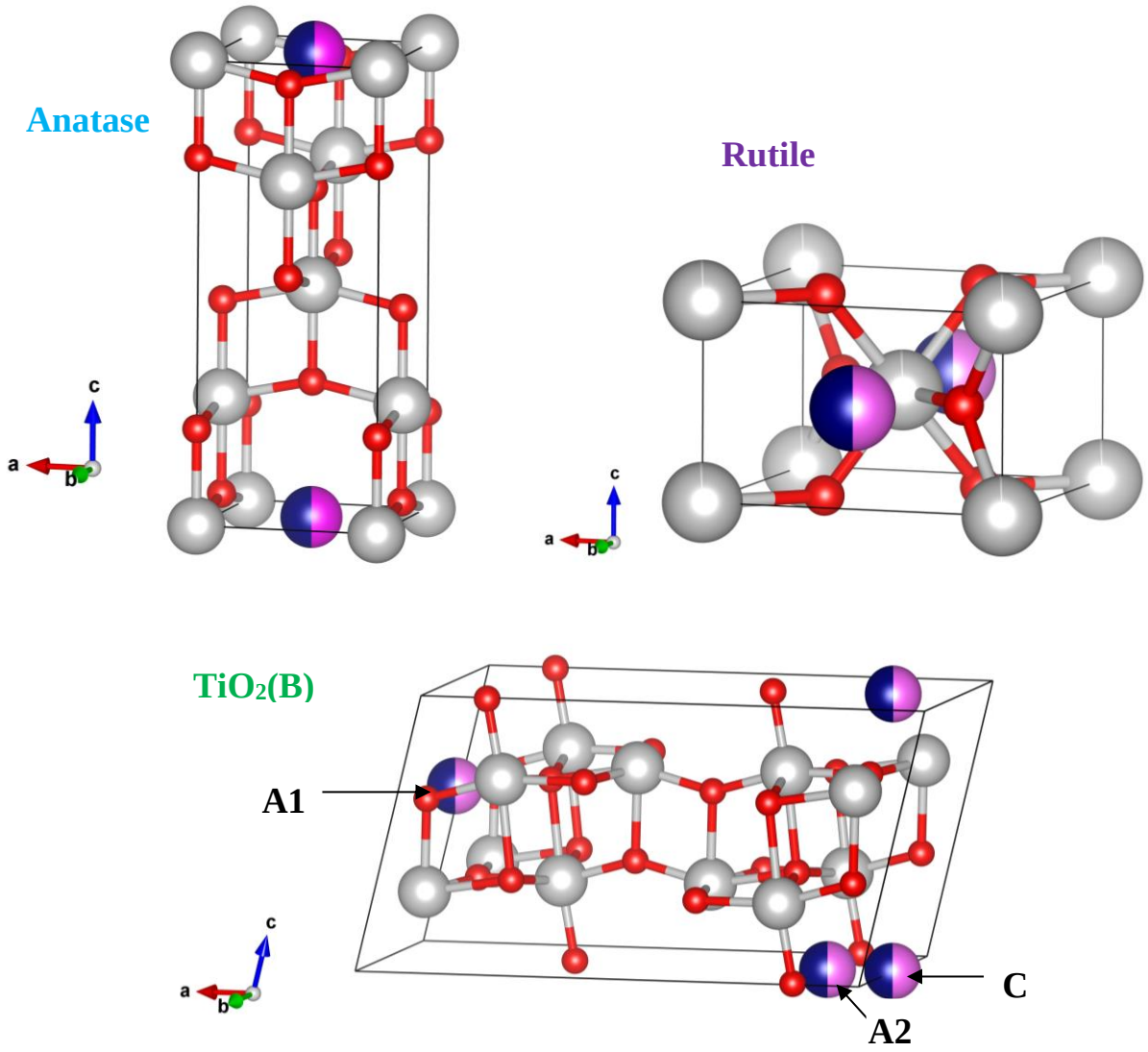

Fig. 3. Possible Li/Na intercalation sites in anatase TiO_2, rutile TiO_2 and TiO_2(B). Only the octahedral sites are shown for anatase and rutile. Red, silver, pink and blue spheres represent O, Ti, Li and Na atoms, respectively.

Various experimental and computational studies have reported that the intercalated ions in do not sit perfectly sit at the centre of the O_6 octahedra for anatase[15,54] and rutile[25], or the C site in TiO_2(B)[43]. The energetic ease for such displacements to occur is a measure of the mobility of Li and Na in these materials. Before calculating the intercalation energies and properties

with the sX functional, we first begin by probing the lowest energy intercalation sites, taking into account displacements, using GGA.

For anatase, displacements were tested along the *c* direction from the energetically stable octahedral intercalation sites. Our calculations confirmed that for Li, a small displacement of ~0.3 Å is the most energetically stable, although it is only 0.01 eV more stable than the centre of the octahedra. This is in good agreement with displacements measured from neutron diffraction[54] and molecular dynamics[55]. For Na, a slightly larger displacement of ~0.4 Å was preferred. Similar results have been reported using GGA[29], where small displacements were measured for Li and larger displacements were observed for Na and Mg. It is noted that the displacements up to these optimised values have the same energies as the central octahedral sites, which once again confirms the relative ease of Li and Na diffusion in TiO_2. Similar displacements are also known occur in rutile[25,56]. Our calculations show an optimal displacement of ~0.5 Å for Li along the *c* direction. Interestingly, there was an energy penalty for displacement of Na away from the octahedra centre, perhaps suggesting a lack mobility for Na in this polymorph, in agreement with the poorer electrochemical performance reported for sodiated rutile[14].

There is some debate in the literature over the lowest energy intercalation site in TiO_2(B) at the dilute limit. The energies calculated in this work for neutral Li and Na at the C, A1 and A2 sites, with respect to the lowest energy site, are listed in Table 2. On the basis of our results, the C site is clearly the lowest energy site (at the dilute limit) for both Li and Na. This is in agreement with a number of previous experimental and DFT studies for Li intercalation[27,29,43,57]. However, it must be noted that there is also a selection of computational studies that predict that the C site is not the most energetically favourable[27,28,58], contrary to neutron diffraction experiments[57]. To the best of our knowledge, the Na intercalation sites in

TiO_2(B) have only once been studied in detail in the literature[29], where it was reported that the C site was the most stable site. Similar to anatase and rutile, off-centre displacements for the intercalating ions in TiO_2(B) have been reported experimentally[57] and computationally[43]. A small energy gain was also observed in this work for displacements in the *b* direction of 0.3 and 0.2 Å for Li and Na, respectively.

Table 2. Relative energies for the most stable Li and Na intercalation sites in TiO_2(B).

Site	Coordinates	Wyckoff	Li *E* (eV)	Na *E* (eV)
C	0.0 0.5 0.0	2b	0	0
A1	0.95 0.50 0.62	4i	0.10	0.07
A2	0.13 0.50 0.00	4i	0.10	0.03

3.3. Li/Na insertion energetics and voltages

Now that the lowest energy intercalation sites have been identified, we use GGA and sX hybrid functional calculations to determine the defect formation/intercalation energies for Li and Na at a composition of x(Li/Na) = 0.03 in the three TiO_2 polymorphs. The calculated energies are plotted against the E_F in Fig. 4. The E_F ranges in the plots in Fig. 4 are determined by the appropriate GGA or sX calculated band-gap of the material, as discussed in Section 3.1. In the vast majority of studies concerning the calculation of intercalation energies using DFT methods, only simplistic defect formation energy equations are considered and usually only neutral defects are considered. In this study, we consider both the neutral and 1+ states of the intercalating ions, so that we can also analyse the charge transition levels for Li and Na in these materials.

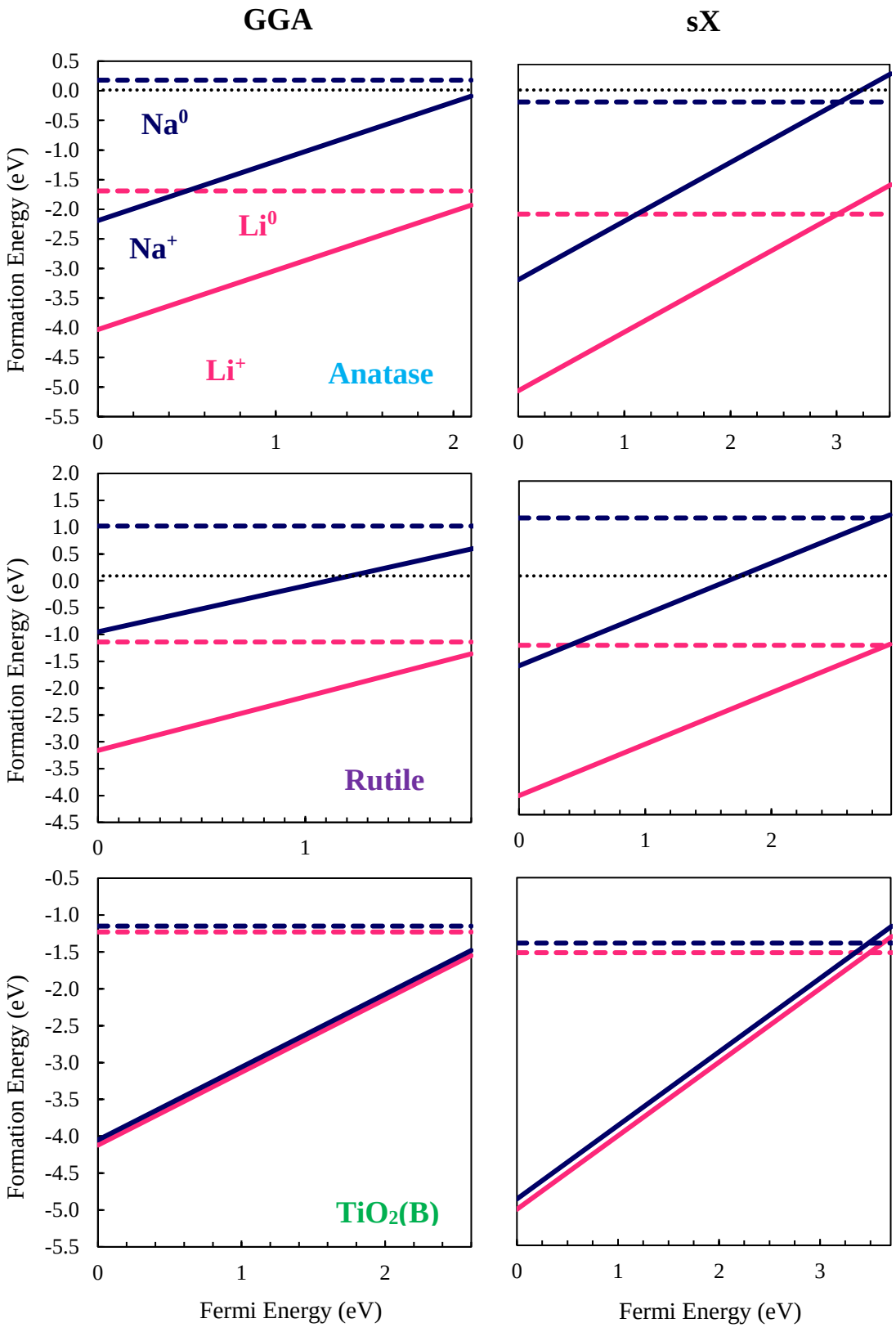

Fig. 4. Defect formation energies for Li and Na intercalation in anatase, rutile and TiO_2(B) calculated using GGA and sX at the metal-rich limit. The top of the valence band is represented by a Fermi energy of 0 eV and Fermi energies are plotted based on the calculated band gaps.

As we can see from Fig. 4, the majority of the energies are negative which means that for the majority of cases, Li/Na insertion is energetically favoured, compared to metal plating. By plotting the GGA energies against the GGA band-gap, it is clear to see one of the main weaknesses of this functional. The GGA results show that the charged intercalating ions dominate the entirety of the Fermi energy ranges, meaning that the 1+/0 charge transition does not occur as a result of the significant band-gap underestimation. Whereas with the more accurate reproduction of the TiO_2 polymorph band-gaps from the sX functional, we now see both the neutral and 1+ charge states occupying sections of the Fermi energy ranges with the charge transition occurring close to the conduction band minimum (CBM) in all cases, as would be expected. Similar results were found for oxygen vacancy calculations in rutile, where both the neutral and 1+ oxygen vacancy charge states were predicted to be unstable with GGA and stable with the HSE hybrid functional[49].

It is common for hybrid functionals to predict lower formation energies for donor defects compared to standard functionals such as GGA. This has been shown several times for defect studies of rutile TiO_2 with HSE[49,50] and sX[34]. Our results are no exception, with the energies for Li^+ and Na^+ in all three polymorphs being lowered by ~1 eV using sX, compared to GGA. However, the picture for the intercalation energies (neutral defects) is not so clear. For Li and Na in anatase and TiO_2(B), in going from GGA to sX, the intercalation energies become more negative, or in the case of Na in anatase, they move from a positive or a negative value. These results agree well with the underestimation of intercalation energies, compared to experiment, sometimes associated with GGA[30,59-61]. However, for rutile, the sX calculated Na and Li intercalation energies are almost identical to the values from GGA. This illustrates that GGA intercalation energy underestimation is not always solved by hybrid functional techniques and/or that the underestimation is structurally dependant. However, it must be noted that

structural dependency is a common issue for DFT functionals, including GGA, so this cannot be considered a major drawback for the sX functional.

We can convert our intercalation energies to average equilibrium voltages, $\bar{V}$, using the following equation:

$$\bar{V} = \frac{-\Delta G}{(n_2 - n_1)F} \qquad (2)$$

where ΔG is the difference in Gibbs free energy between the de-lithiated/sodiated phase (charged state) and lithiated/sodiated phase (discharged state) and F is the Faraday constant. This calculation can be simplified by the fact that ΔG can be approximated by the internal (potential) energy change per intercalated Li or Na (i.e. the intercalation energy) because the vibrational and configurational entropy contributions to the cell voltage at room temperature are expected to be small. The calculated voltages are presented in Table 3.

Table 3. Li and Na intercalation voltages for the three TiO_2 polymorphs, calculated using GGA and sX. Voltages have been omitted for the predicted non-intercalating species.

Polymorph	GGA Li (V)	sX Li (V)	GGA Na (V)	sX Na (V)
Anatase	1.69	2.05	-	0.14
Rutile	1.14	1.20	-	-
TiO_2(B)	1.23	1.52	1.15	1.39

It is has been both experimentally and computationally shown that anatase will readily incorporate Li[8-10,15]. Experimentally, anatase is generally considered to be the most feasible TiO_2 polymorph for Li incorporation because of its three dimensional open structure[13] and this is in perfect agreement with our results. Li in anatase has been shown to have an initial

intercalation voltage of ~2.5 V, which then rapidly falls to 1.78 V by x(Li) = 0.05[15]. Our sX Li intercalation voltage of 2.05 V is in agreement with this, however, our GGA value of 1.69 V is too small. For Na in anatase, GGA predicts a positive intercalation, meaning that its incorporation is thermodynamically unfavourable, using sX, a small voltage of 0.14 V is obtained. This low voltage is to be expected given the increased ionic radius of Na (1.02 Å) compared to Li (0.76 Å)[62]. It also supports the experimental and computational evidence for the difficulty of intercalating Na into anatase, particularly for bulk samples[11-13,29]. Xiong et al.[11] proposed that crystalline TiO_2 cannot support Na intercalation above 0.8 V, which agrees well with our findings. To the best of our knowledge, Na intercalation into TiO_2 nanostructures or surfaces has not been considered computationally, but this is certainly a topic of interest and it should allow us to see the real difference between the intercalation voltages in the bulk and nanostructured materials. Alternatively, amorphous TiO_2 has been computationally considered for Li and Na intercalation[29]. Using GGA, Legrain et al.[29] showed that the lowest energy sites in their amorphous model have great potential for Li and Na incorporation with intercalation energies as large as -3.06 and -2.54 eV for Li and Na, respectively, higher than any values reported for anatase, rutile and TiO_2(B).

Li intercalation in rutile is also thermodynamically favourable, albeit to a lesser extent than anatase or TiO_2(B). This is again, in excellent agreement with experimental findings, where rutile is known to incorporate less Li than both anatase[18] and TiO_2(B)[22]. Our values for Li intercalation in rutile are in reasonable agreement with the experimental voltages of 1.4 and 1.5 V[63]. It is noteworthy that a previously reported GGA intercalation energy for Li intercalation in rutile (-1.70 eV[29]) is considerably larger than both our GGA and sX values and indeed, the experimental values. This is also the case for a number of intercalation energies in the same study. The reason for the overestimations in REF. 29 is not entirely clear, but it is likely to be an unfortunate result of the different simulation parameters used in different studies

e.g. cell sizes, correction procedures, pseudopotentials and DFT codes. Na intercalation in rutile is unfavoured using both the GGA and sX functionals, in agreement with previous computational work[29]. Experimentally, sodiated rutile can be formed, but its electrochemical activity is poor[14]. However, as discussed previously, sodiated rutile microspheres have shown some promising results[21]. On the basis of our results, out of the three bulk TiO_2 polymorphs considered, rutile is the worst choice as an anode material in both Li and Na batteries.

For TiO_2(B), the calculated Li and Na intercalation voltages are somewhat similar, although the underestimation from GGA is still present. This suggests that, unlike the other two polymorphs considered, TiO_2(B) can readily incorporate both Li and Na. Experimental voltages for Li-intercalated TiO_2(B) range from 1.75 to 2.00 V for $x < 0.125$[64] and ~1.5 V for nanostructures with $x = 0.5$[64]. Our sX value of 1.52 V is in good agreement with these ranges, although it is still somewhat of an underestimate, it is a significant improvement on our GGA result. Computationally, GGA intercalation energies of up to -2.06 eV[29] and intercalation voltages of up to -1.64 V[43] have been reported. The significant spread of data for DFT determined intercalation energies and voltages in the literature further asserts the importance of the comparative study carried out in this work. According to our results, TiO_2(B) is the only bulk polymorph that will readily incorporate Na and therefore must be proposed as the best anode material for Na-ion batteries for the three materials considered. This agrees with several electrochemical studies which show the potential of TiO_2(B) in Na-ion batteries[23,24,65]. Voltages of less than 1.5 V have been reported for nanostructured TiO_2(B)[23,24,65], which are similar to our calculated of 1.39 V. These voltages values are also higher than those reported for Na-intercalated anatase and rutile, further supporting our argument that TiO_2(B) is the best candidate for application in Na-ion batteries. Favourable Na intercalation in TiO_2(B) (-1.96 eV) was also shown previously using GGA calculations[29], albeit again with a dramatic overestimation.

3.4. Electronic structures

It is well-known that GGA cannot correctly reproduce the electronic structures of Li-/Na-intercalated TiO_2 as a consequence of the self-interaction error[15]. While GGA+*U* can correct for this error and correctly localise the excess charge on one nearby Ti site, it can still be subject to band-gap error and, as discussed, the *U* parameter is sometimes fitted for one desired purpose. To account for these problems, we calculate the spin-polarised PDOS using the sX functional. The results are presented in Fig. 5. As the results for the Na-intercalated polymorphs are very similar to their Li-intercalated counterparts, with almost identical defect state positions and band-gaps, we only present the electronic structures of the Li-intercalated polymorphs here. Please note that the Li s states are negligible in the energy range used in Fig. 5.

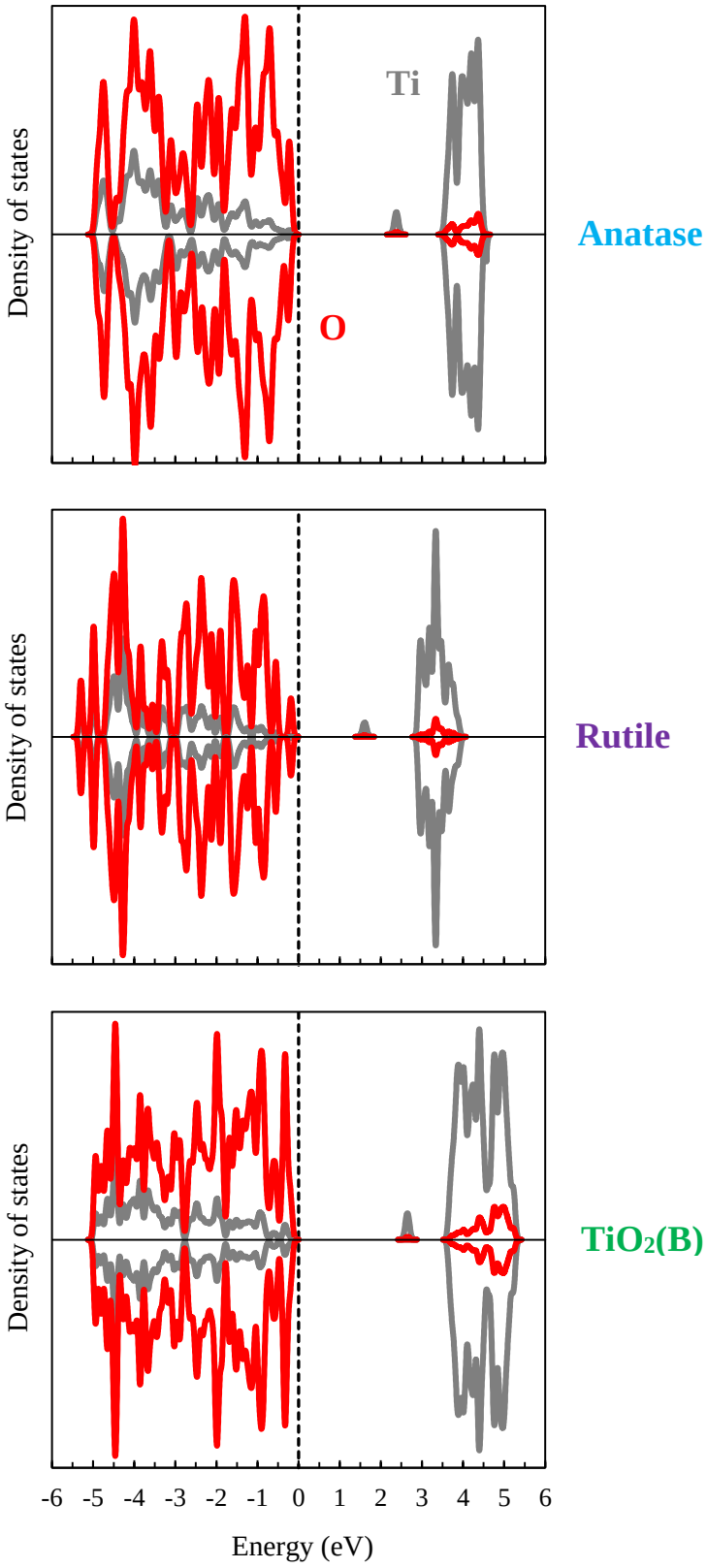

Fig. 5. PDOS of the three Li-intercalated TiO_2 polymorphs calculated using the sX functional.

Generally, in GGA calculations of TiO_2, the excess charge from intercalating Li and Na ions lies at the bottom of the conduction band, with no defect states produced in the band-gap[15,25,27]. In such calculations, localisation fails and the charge is delocalised over all the Ti ions in the cell. From Fig. 5, it is clear that the sX functional corrects these issues, as a gap state is formed in each of the PDOS plots, resulting from the excess Li charge. This is in agreement with the defect states found in X-ray photoelectron spectroscopy (XPS) studies of anatase[66,67] and rutile[68]. In these calculations, the excess charge is now strongly localised on a nearby Ti site, effectively producing a Ti^{3+} ion, in agreement with previous GGA+U[15,27], HSE[69] and Hartree-Fock[26] calculations. The three defect states are all around 1 eV below the conduction band minimum, again, similar to previous results[15,27,69]. It should be noted that a recent study of Li, Na and Mg intercalation in TiO_2 reported that the defect states and correct charge localisation can in fact be achieved at the GGA level[29]. This was achieved using "tuned" localised basis sets and norm-conserving pseudopotentials. However, it is certain that further investigation is required to verify these findings.

4. Conclusions

By employing the sX hybrid functional, we have been able to calculate accurate defect energies, intercalation voltages and electronic structures for Li- and Na-intercalated anatase, rutile and TiO_2(B). Hybrid functionals have been widely applied to numerous types of materials due to their ability to more reliably reproduce various material properties, compared to standard local-density functionals which are subject to self-interaction issues. However, the use of hybrid functionals for the calculation of battery material properties is still somewhat limited.

The GGA functional has been reported to underestimate intercalation energies and this is further supported by our sX and GGA comparative calculations of Li and Na intercalation in

the three studied TiO_2 polymorphs. Using sX, Li intercalation is most energetically preferred in anatase, while Na intercalation is most feasible for TiO_2(B). All intercalation processes are shown to be thermodynamically favourable, with the exception of Na in rutile. Intercalation voltages are generally in good agreement with experiment. Excess charge localisation at individual Ti sites is confirmed by sX DOS calculations and significantly improved band-gap prediction is shown, compared to GGA. Our hybrid calculations have also provided new physical insights into these materials, such as the existence of an energy penalty for Na off-centring in rutile, indicative of the poor electrochemical performance for this sodiated material.

Using sX allows us to abolish many of the errors associated with GGA and GGA+*U*, meaning that we can establish a more accurate reference point for future calculations and circumvent some of the typical arguments and confusion associated with the comparisons between local-density and post-density functional methods, and their ad hoc corrections. However, it is important to state that hybrid functional calculations are clearly not appropriate for all calculations on Li-ion battery materials. They are still limited by computational expense and are not viable for calculations with very large supercells, which are often required for transport property or interface calculations.

ACKNOWLEDGEMENTS

The authors thank the Engineering and Physical Sciences Research Council for funding from EPSRC grant EP/M009297.

REFERENCES

(1) Tarascon, J.-M.; Armand, M. Issues and Challenges Facing Rechargeable Lithium Batteries. *Nature* **2001**, *414*, 359−367.

(2) Armand, M.; Tarascon, J.-M. Building Better Batteries. *Nature* **2008**, *451*, 652−657.

(3) Bruce, P. G.; Scrosati, B.; Tarascon, J.-M. Nanomaterials for Rechargeable Lithium Batteries. *Angew. Chem. Int. Ed.* **2008**, *47*, 2930−2946.

(4) Islam, M. S.; Fisher, C. A. J. Lithium and Sodium Battery Cathode Materials: Computational Insights into Voltage, Diffusion and Nanostructural Properties. *Chem. Soc. Rev.* **2014**, *43*, 185−204.

(5) Huang, S. Y.; Kavan, L.; Exnar, I.; Grätzel, M. Rocking Chair Lithium Battery Based on Nanocrystalline TiO_2 (Anatase). *J. Electrochem. Soc.* **1995**, *142*, L142−L144.

(6) Jiang, C. H.; Wei, M. D.; Qi, Z. M.; Kudo, T.; Honma, I.; Zhou, H. S. Particle Size Dependence of the Lithium Storage Capability and High Rate Performance of Nanocrystalline Anatase TiO_2 Electrode. *J. Power Sources* **2007**, *166*, 239−243.

(7) Goodenough, J. B.; Kim, Y. Challenges for Rechargeable Li Batteries. *Chem. Mater.* **2010**, *22*, 587−603.

(8) Myung, S.-T.; Kikuchi, M.; Yoon, C. S.; Yashiro, H.; Kim, S.-J.; Sun, Y.-K.; Scrosati, B. Black Anatase Titania Enabling Ultra High Cycling Rates for Rechargeable Lithium Batteries. *Energy Environ. Sci.* **2013**, *6*, 2609−2614.

(9) Wagemaker, M.; Borghols, W. J. H.; Mulder, F. M. Large Impact of Particle Size on Insertion Reactions. A Case for Anatase Li_xTiO_2. *J. Am. Chem. Soc.* **2007**, *129*, 4323−4327.

(10) Deng, D.; Kim, M. G.; Lee, J. Y.; Cho, J. Green Energy Storage Materials: Nanostructured TiO_2 and Sn-Based Anodes for Lithium-Ion Batteries. *Energy Environ. Sci.* **2009**, *2*, 818−837.

(11) Xiong, H.; Slater, M. D.; Balasubramanian, M.; Johnson, C. S.; Rajh, T. Amorphous TiO_2 Nanotube Anode for Rechargeable Sodium Ion Batteries. *J. Phys. Chem. Lett.* **2011**, *2*, 2560−2565.

(12) Xu, Y.; Loftabad, E. M.; Wang, H.; Farbod, B.; Xu, Z.; Kohandehghan, A.; Mitlin, D. Nanocrystalline anatase TiO_2: A New Anode Material for Rechargeable Sodium Ion Batteries. *Chem. Commun.* **2013**, *49*, 8973−8975.

(13) Kim, K.-T.; Ali, G.; Chung, K. Y.; Yoon, C. S.; Yashiro, H.; Sun, Y.-K.; Lu, J.; Amine, K.; Myung, S.-T. Anatase Titania Nanorods as an Intercalation Anode Material for Rechargeable Sodium Batteries. *Nano Lett.* **2014**, *14*, 416−422.

(14) Su, D.; Dou, S.; Wang, G. Anatase TiO_2: Better Anode Material Than Amorphous and Rutile Phases of TiO_2 for Na-Ion Batteries. *Chem. Mater.* **2015**, *27*, 6022−6029.

(15) Morgan, B. J.; Watson, G. W. GGA+*U* Description of Lithium Intercalation into Anatase TiO_2. *Phys. Rev. B* **2010**, *82*, 144119.

(16) Wagemaker, M.; Kentgens, A. P. M.; Mulder, F. M. Equilibrium Lithium Transport Between Nanocrystalline Phases in Intercalated TiO_2 Anatase. *Nature* **2002**, *418*, 397−399.

(17) Wagemaker, M.; Borghols, W. J. H.; van Eck, E. R. H.; Kentgens, A. P. M.; Kearley, G. J.; Mulder, F. M. The Influence of Size on Phase Morphology and Li-Ion Mobility in Nanosized Lithiated Anatase TiO_2. *Chem.-Eur. J.* **2007**, *13*, 2023−2028.

(18) Milne, N. A.; Skyllas-Kazacos, M.; Luca, V. Crystallite Size Dependence of Lithium Intercalation in Nanocrystalline Rutile. *J. Phys. Chem. C* **2009**, *113*, 12983−12995.

(19) Chen, J. S.; Lou, X. W. The Superior Lithium Storage Capabilities of Ultra-Fine Rutile TiO_2 Nanoparticles. *J. Power Sources* **2010**, *195*, 2905−2908.

(20) Hu, Y.-S.; Kienle, L.; Guo, Y.-G.; Maier, J. High Lithium Electroactivity of Nanometer-Sized Rutile TiO_2. *Adv. Mater.* **2006**, *18*, 1421−1426.

(21) Zhang, Y.; Pu, X.; Yang, Y.; Zhu, Y.; Hou, H.; Jing, M.; Yang, X.; Chen, J.; Ji, X. An Electrochemical Investigation of Rutile TiO_2 Microspheres Anchored by Nanoneedle Clusters for Sodium Storage. *Phys. Chem. Chem. Phys.* **2015**, *17*, 15764−15770.

(22) Armstrong, A. R.; Armstrong, G.; Canales, J.; Garciá, R.; Bruce, P. G. Lithium-Ion Intercalation into TiO_2-B Nanowires. *Adv. Mater.* **2005**, *17*, 862−865.

(23) Huang, J. P.; Yuan, D. D.; Zhang, H. Z.; Cao, Y. L.; Li, G. R.; Yang, H. X.; Gao, X. P. Electrochemical Sodium Storage of TiO_2(B) Nanotubes for Sodium Ion Batteries. *RSC Adv.* **2013**, *3*, 12593−12597.

(24) Chen, C.; Wen, Y.; Hu, X.; Ji, X.; Yan, M.; Mai, L.; Hu, P.; Shan, B.; Huang, Y. Na^+ Intercalation Pseudocapacitance in Graphene-Coupled Titanium Oxide Enabling Ultra-Fast Sodium Storage and Long-Term Cycling. *Nat. Commun.* **2015**, *6*, 6929.

(25) Koudriachova, M. V.; Harrison, N. M.; de Leeuw, S. W. Density-Functional Simulations of Lithium Intercalation in Rutile. *Phys. Rev. B* **2002**, *65*, 235423.

(26) Stashans, A.; Lunell, S.; Bergström, R.; Hagfeldt, A.; Lindquist, S.-E. Theoretical Study of Li Intercalation in Rutile and Anatase. *Phys. Rev. B* **1996**, *53*, 159−170.

(27) Morgan, B. J.; Madden, P. A. Lithium Intercalation into TiO_2(B): A Comparison of LDA, GGA, and GGA+*U* Density Functional Calculations. *Phys. Rev. B* **2012**, *86*, 035147.

(28) Dalton, A. S.; Belak, A. A.; Van der Ven, A. Thermodynamics of Lithium in TiO_2(B) from First Principles. *Chem. Mater.* **2012**, *24*, 1568−1574.

(29) Legrain, F.; Malyi, O.; Manzhos, S. Insertion Energetics of Lithium, Sodium, and Magnesium in Crystalline and Amorphous Titanium Dioxide: A Comparative First-Principles Study. *J. Power Sources* **2015**, *278*, 197−202.

(30) Zhou, F.; Cococcioni, M.; Marianetti, C. A.; Morgan, D.; Ceder, G. First-Principles Prediction of Redox Potentials in Transition-Metal Compounds with LDA+*U*. *Phys. Rev. B* **2004**, *70*, 235121.

(31) Clark, S. J.; Robertson, J.; Lany, S.; Zunger, A. Intrinsic Defects in ZnO Calculated by Screened Exchange and Hybrid Density Functionals. *Phys. Rev. B* **2010**, *81*, 115311.

(32) Clark, S. J.; Robertson, J. Screened Exchange Density Functional Applied to Solids. *Phys. Rev. B* **2010**, *82*, 085208.

(33) Li, H.; Guo, Y.; Robertson, J. Calculation of TiO_2 Surface and Subsurface Oxygen Vacancy by the Screened Exchange Functional. *J. Phys. Chem. C* **2015**, *119*, 18160−18166.

(34) Lee, H.-Y.; Clark, S. J.; Robertson, J. Calculation of Point Defects in Rutile TiO_2 by the Screened-Exchange Hybrid Functional. *Phys. Rev. B* **2012**, *86*, 075209.

(35) Clark, S. J.; Robertson, J. Calculation of Semiconductor Band Structures and Defects by the Screened Exchange Density Functional. *Phys. Stat. Sol. B* **2011**, *248*, 537−546.

(36) Dawson, J. A.; Guo, Y.; Robertson, J. Energetics of Intrinsic Defects in NiO and the Consequences for its Resistive Random Access Memory Performance. *Appl. Phys. Lett.* **2015**, *107*, 122110.

(37) Segall, M. D.; Lindan, P. J. D.; Probert, M. J.; Pickard, C. J.; Hasnip, P. J.; Clark, S. J.; Payne, M. J. First-Principles Simulation: Ideas, Illustrations and the CASTEP Code. *J. Phys.: Condens. Matter* **2005**, *14*, 2717–2744.

(38) OPIUM pseudopotential package, http://opium.sourceforge.net.

(39) Perdew, J. P.; Burke, K.; Ernzerhof, M. Generalized Gradient Approximation Made Simple. *Phys. Rev. Lett.* **1996**, *77*, 3865–3868.

(40) Burdett, J. K.; Hughbanks, T.; Miller, G. J.; Richardson Jr., J. W.; Smith, J. V. Structural-Electronic Relationships in Inorganic Solids: Powder Neutron Diffraction Studies of the Rutile and Anatase Polymorphs of Titanium Dioxide at 15 and 295 K. *J. Am. Chem. Soc.* **1987**, *109*, 3639–3646.

(41) Feist, T. P.; Davies, P. K. The Soft Chemical Synthesis of TiO_2(B) from Layered Titanates. *J. Solid State Chem.* **1992**, *101*, 275–295.

(42) Morgan, B. J.; Watson, G. W. Intrinsic n-type Defect Formation in TiO_2: A Comparison of Rutile and Anatase from GGA+*U* Calculations. *J. Phys. Chem. C* **2010**, *114*, 2321−2328.

(43) Arrouvel, C.; Parker, S. C.; Islam, M. S. Lithium Insertion and Transport in the TiO_2-B Anode Material: A Computational Study. *Chem. Mater.* **2009**, *21*, 4778−4783.

(44) Scanlon, D. O.; Dunnill, C. W.; Buckeridge, J.; Shevlin, S. A.; Logsdail, A. J.; Woodley, S. M.; Catlow, C. R. A.; Powell, M. J.; Palgrave, R. G.; Parkin, I. P.; Watson, G. W.; Keal, T.

W.; Sherwood, P.; Walsh, A.; Sokol, A. A. Band Alignment in Rutile and Anatase TiO_2. *Nat. Mater.* **2013**, *12*, 798−801.

(45) Zhu, T.; Gao, S.-P. The Stability, Electronic Structure, and Optical property of TiO_2 Polymorphs. *J. Phys. Chem. C* **2014**, *118*, 11385−11396.

(46) Wang, Y.; Zhang, H.; Liu, P.; Yao, X.; Zhao, H. Engineering the Band Gap of Bare Titanium Dioxide Materials for Visible-Light Activity: A Theoretical Prediction. *RSC Adv.* **2013**, *3*, 8777−8782.

(47) Chen, C.; Hu, X.; Zhang, B.; Miao, L.; Huang, Y. Architectural Design and Phase Engineering of N/B-Codoped TiO_2(B)/Anatase Nanotube Assemblies for High-Rate and Long-Life Lithium Storage. *J. Mater. Chem. A* **2015**, *3*, 22591−22598.

(48) D'Elia, D. Elaboration and Study of TiO_2 Nanostructures for Hydrogen Generation via Photolysis of Water. PhD Thesis. École Nationale Supérieure des Mines de Paris, **2011**.

(49) Janotti, A.; Varley, J. B.; Rinke, P.; Umezawa, N.; Kresse, G.; Van de Walle, C. G. Hybrid Functional Studies of the Oxygen Vacancy in TiO_2. *Phys. Rev. B* **2010**, *81*, 085212.

(50) Bjørheim, T. S.; Kuwabara, A.; Norby T. Defect Chemistry of Rutile TiO_2 from First Principles Calculations. *J. Phys. Chem. C* **2013**, *117*, 5919−5930.

(51) Chen, H.; Dawson, J. A. Molecular Oxygen as Charge-Compensating and Magnetic Centers in Anatase TiO_2. *Phys. Rev. Appl.* **2015**, *3*, 064011.

(52) Chen, H.; Dawson, J. A. Nature of Nitrogen-Doped Anatase TiO_2 and the Origin of its Visible-Light Activity. *J. Phys. Chem. C* **2015**, *119*, 15890−15895.

(53) Brohan, L.; Marchand, R. Properties Physiques des Bronzes M_xTiO_2 (B). *Solid State Ionics* **1983**, *9 & 10*, 419−424.

(54) Wagemaker, M.; Kearley, G. J.; van Well, A. A.; Mutka, H.; Mulder, F. M. Multiple Lithium Positions Inside Oxygen Octahedra Lithiated TiO_2 Anatase. *J. Am. Chem. Soc.* **2003**, *125*, 840−848.

(55) Kerisit, S.; Rosso, K. M.; Yang, Z.; Liu, J. Dynamics of Coupled Lithium/Electron Diffusion in TiO_2 Polymorphs. *J. Phys. Chem. C* **2009**, *113*, 20998−21007.

(56) Koudriachova, M. V.; Harrison, N. M.; de Leeuw, S. W. Diffusion of Li-Ions in Rutile. An Ab Initio Study. *Solid State Ionics* **2003**, *157*, 35−38.

(57) Armstrong, A. R.; Arrouvel, C.; Gentili, V.; Parker, S. C.; Islam, Bruce, M. S.; Bruce, P. G. Lithium Coordination Sites in Li_xTiO_2(B): A Structural and Computational Study. *Chem. Mater.* **2010**, *22*, 6426−6432.

(58) Panduwinata, D.; Gale, J. D. A First Principles Investigation of Lithium Intercalation in TiO_2-B. *J. Mater. Chem.* **2009**, *19*, 3931−3940.

(59) Ceder, G. Opportunities and Challenges for First-Principles Materials Design and Applications to Li Battery Materials. *MRS Bull.* **2010**, *35*, 693−701.

(60) Ceder, G.; Hautier, G.; Jain, A.; Ong, S. P. Recharging Lithium Battery Research with First-Principles Methods. *MRS Bull.* **2011**, *36*, 185−191.

(61) Dawson, J. A.; Tanaka, I. Li Intercalation into a β-MnO_2 Grain Boundary. *ACS Appl. Mater. Interfaces* **2015**, *7*, 8125−8131.

(62) Shannon, R. D. Revised Effective Ionic Radii and Systematic Studies of Interatomic Distances in Halides and Chalcogenides. *Acta Crystallogr.* **1976**, *32*, 751−767.

(63) Macklin, W. J.; Neat, R. J. Performance of Titanium Oxide-Based Cathodes in a Lithium Polymer Electrolyte Cell. *Solid State Ionics* **1992**, *53–56*, 694–700.

(64) Armstrong, A. R.; Armstrong, G.; Canales, J.; Bruce, P. G. TiO_2-B Nanowires. *Angew. Chem. Int. Ed.* **2004**, *43*, 2286−2288.

(65) Wu, L.; Bresser, D.; Buchholz, B.; Passerini, S. Nanocrystalline TiO_2(B) as Anode Material for Sodium-Ion Batteries. *J. Electrochem. Soc.* **2015**, *162*, A3052−A3058.

(66) Södergren, S.; Siegbahn, H.; Rensmo, H.; Lindström, H.; Hagfeldt, A.; Lindquist, S.-E. Lithium Intercalation in Nanoporous Anatase TiO_2 Studied with XPS. *J. Phys. Chem. B* **1997**, *101*, 3087−3090.

(67) Richter, J. H.; Henningsson, A.; Karlsson, P. G.; Andersson, M. P.; Uvdal, P.; Siegbahn, H.; Sandell, A. Electronic Structure of Lithium-Doped Anatase TiO_2 Prepared in Ultrahigh Vacuum. *Phys. Rev. B* **2005**, *71*, 235418.

(68) Uhl, B.; Hekmatfar, M.; Buchner, F.; Behm, R. J. Interaction of the Ionic Liquid [BMP][TFSA] with Rutile TiO_2(110) and Coadsorbed Lithium. *Phys. Chem. Chem. Phys.* **2016**, *18*, 6618−6636.

(69) Spreafico, C.; VandeVondele, J. Excess Electrons and Interstitial Li Atoms in TiO_2 Anatase: Properties of the (101) Interface. *J. Phys. Chem. C* **2015**, *119*, 15009−15018.